ISSN 0018-1439, High Energy Chemistry, 2024, Vol. 58, No. 3, pp. 281–294. © Pleiades Publishing, Ltd., 2024.

GENERAL ASPECTS

Spin-Dependent Control of Electronic and Magnetic Properties of 3-Alkylthiophene Oligomers and Their Composites with Aromatic Nanoadditives

V. I. Krinichnyi*

Federal Research Center for Problems of Chemical Physics and Medicinal Chemistry, Russian Academy of Sciences, Chernogolovka, Moscow oblast, 142432 Russia

**e-mail: kivi@icp.ac.ru*

Received July 21, 2023; revised January 17, 2024; accepted January 18, 2024

Abstract—The energy and spin parameters of 3-alkylthiophene oligomers and their composites with aromatic hydrocarbons have been calculated. The coexistence of polarons with different degrees of delocalization in the studied compounds has been identified. It has been revealed that the electronic and spin properties of the composites undergo a periodic change initiated by the interaction of the oligomers with aromatic nanoadditives. The anisotropic parameters of spin Hamiltonians have been obtained for the systems under study, and their high-resolution EPR spectra have been calculated.

Keywords: oligomer, polyaromatic nanoadditives, polaron, polythiophene, radical, hyperfine coupling, density functional theory (DFT), electron paramagnetic resonance (EPR)

DOI: 10.1134/S0018143924700085

INTRODUCTION

Organic polymer semiconductors are widely used to create solar cells, chemical sensors, field-effect transistors, and other molecular devices [1, 2]. Various regioregular poly(3-alkylthiophenes) (P3AT) with different side substituents and other conjugated polymers [3] are commonly used as active matrices of donor–acceptor complexes, while fullerene-containing [4] and fullerene-free [5] compounds are counterions. The interaction of complexes, for example, with light photons leads to the generation of excitons in them. During the decay of these quasi-particles, an electron is separated from the polymer chain and a local topological distortion known as polaron is formed on it, being several monomers in size and carrying an elementary charge and a half-integer spin oriented either in the direction (+1/2) or against the direction (−1/2) of external magnetic field. In this case, the aromatic form of the polymer is replaced by the quinoid one. Such a conformational transition is accompanied, in particular, by a decrease in the dihedral/torsion angle with the subsequent structuring of nearby macromolecules bearing similar charge carriers. The hyperfine interaction of polaron spins with their microenvironment in such a composite increases, due to which the dimensionality and speed of intermolecular spin dynamics increase. The spin nature of charge carriers determines the specificity of most processes occurring in polymeric donor–acceptor compounds, depending on their spin state, spin-to-spin coupling, and position in an external magnetic field. This makes it possible to adjust the bandgap and thereby control the thermal transfer of generated charge from the valence band to the conduction band of the composite by simply changing its spin state, for example, by the action light.

All processes occurring in polymer systems depend on their morphology and, in addition, on the structure and donor–acceptor properties of their ingredients. They can be regulated, in particular, by the effects of spin–photon and/or spin–spin exchange interaction on their electronic and spin parameters. Since these processes involve spin charge carriers, the direct technique of electron paramagnetic resonance (EPR) has found wide application for their study [6, 7].

Previous studies [8, 9] have shown that the introduction of small Q2D aromatic molecules into polymer donor–acceptor composites significantly improves their functional properties. It was found that such additives play the role of crystallization sites in the polymer matrix of composites; the crystallization increases the structuring of their matrix and thereby enhances the stability of spin charge carriers generated in them. This paper considers the results of a study on the effect of both structural parameters of P3AT oligomers with various side alkyl substituents and the spin–spin exchange interaction with their microenvironment on the anisotropic parameters of the spin Hamiltonian of polaron charge carriers. The possibility of

controlling the spin state and electronic properties of the studied oligomers by modifying them with polycyclic aromatic hydrocarbons has been demonstrated.

METHODS AND PROCEDURES

Compounds Used in the Study

The following 3-alkylthiophene oligomers (P3AT, see Fig. 1) with various alkyl substituents A ≡ R = C_mH_{2m+1} were investigated: poly(3-hydrothiophene) (P3HyT, $m = 0$), poly(3-methylthiophene) (P3MeT, $m = 1$), poly(3-ethylthiophene) (P3EtT, $m = 2$), poly(3-butylthiophene) (P3BuT, $m = 4$), poly(3-hexylthiophene) (P3HxT, $m = 6$), poly(3-octylthiophene) (P3OcT, $m = 8$), poly(3-decylthiophene) (P3DeT, $m = 10$), and poly(3-dodecylthiophene) (P3DoT, $m = 12$) with the number of monomers n in aromatic and quinoid conformations in the absence and presence of polarons with spin $S = 1/2$ and positive elementary charge $+e$, respectively. In order to analyze the influence of polycyclic aromatic hydrocarbons (PAH) on the electronic and spin properties of P3HyT and P3MeT oligomers, the quasi-one-dimensional (Q1D) polyacenes (PAs) benzene ($n = 1$), naphthalene ($n = 2$), anthracene ($n = 3$), tetracene ($n = 4$), pentacene ($n = 5$), hexacene ($n = 6$), heptacene ($n = 7$), octacene ($n = 8$), nonacene ($n = 9$), and decacene ($n = 10$) were used, as well as quasi-two-dimensional (Q2D) polyaromatic hydrocarbons (PH). These compounds are also shown in Fig. 1 without hydrogen atoms.

DFT Calculation of 3-Alkylthiophene Oligomers

The energy levels of the frontier highest occupied (HOMO) and lowest unoccupied (LUMO) molecular orbitals, E_{HOMO} and E_{LUMO}, respectively, as well as the bandgaps $E_g = E_{LUMO} - E_{HOMO}$ of the above-listed P3AT oligomers and their composites with aromatic additives PA and PH were calculated using the density functional theory (DFT) approximation in the Orca software package (version 5.0.4) [10] with the B3LYP functional. The structure geometry of the studied molecular systems was previously optimized using a parallel data transfer software interface (MPI) to all cores of the computer processor used. The population of electron spins and charge density in the compounds under study were calculated in the Mulliken approximation [11]. Anisotropic and averaged hyperfine spin–spin coupling (HFC) constants and the Landé g-factor were determined using the EPRNMR module with the EPRII basis set for ^{1}H to ^{12}C nuclei, as well as the additional TZVPP basis set for ^{32}S nuclei. To test the effect of the basis set type on the calculated EPR parameters, additional single-point calculations were performed using the def2-TZVPP basis set for all atoms of the compounds used. They showed minor differences in the calculation of all magnetic resonance parameters of the studied systems, as in the case of other polymer donor–acceptor composites [12]. Therefore, all the calculated parameters presented in this work were obtained with the EPRII and TZVPP basis sets, taking into account all possible molecular conformers and atoms of their side substituents. Since no significant influence of the type of basis set on the optimized geometry and magnetic resonance parameters was found, all further calculations were also carried out under the assumption of vacuum. It should be noted that unusual changes in the components of their spin Hamiltonian were recorded for some systems (see below). In this case, multiple appropriate calculations were carried out to establish an unambiguous conclusion. Band structures and orbital configurations were visualized using the Avogadro v.1.2.0 program [13].

DFT Calculation of EPR Spectra of Spin Charge Carriers in 3-Alkylthiophene Oligomers

The calculated hyperfine coupling constants and the principal values of the g-tensor of spin charge carriers obtained by the DFT calculations in the Orca software for the studied oligomers were then used for numerical simulation and visualization of their high-resolution D-band EPR spectra ($\nu_e = \omega_e/2\pi =$ 140 GHz, $B_0 = 4996$ mT) using the EasySpin v.5.2.35 software package [14]. The simulation took into account additional anisotropic field-dependent broadening of the spectra due to unresolved hyperfine splitting (B-strain) of the polaron spin energy level and the distribution of spin Hamiltonian parameters (g-strain). Both broadenings are characterized by a Gaussian distribution. The calculated EPR spectra were compared with those previously obtained experimentally with a millimeter-band EPR spectrometer.

RESULTS AND DISCUSSION

Calculation of the Molecular and Band Structure of 3-Alkylthiophene Oligomers

The inset in Fig. 2 shows the quinoid segments of P3AT polymer chains that accommodate positively and negatively charged polarons induced in the polymer donor–acceptor composite, for example, by its irradiation with light photons. The formation of such spin charge carriers is accompanied by the appearance in the composite bandgap E_g^0 of the corresponding energy sublevels under its lowest unoccupied molecular orbital (LUMO) at a distance E_1 and above its highest occupied molecular orbital (HOMO) at a distance E_2, as shown in Fig. 2. The parameters E_g^0, E_1, and E_2 calculated for P3HyT in the Hartree–Fock approximation were 2.20, 0.71, and 0.61 eV, respectively [15]. The distance between polaron sublevels increases with increasing external magnetic field strength B_0 with a coefficient/slope of 1.175×10^{-7} eV/mT [16].

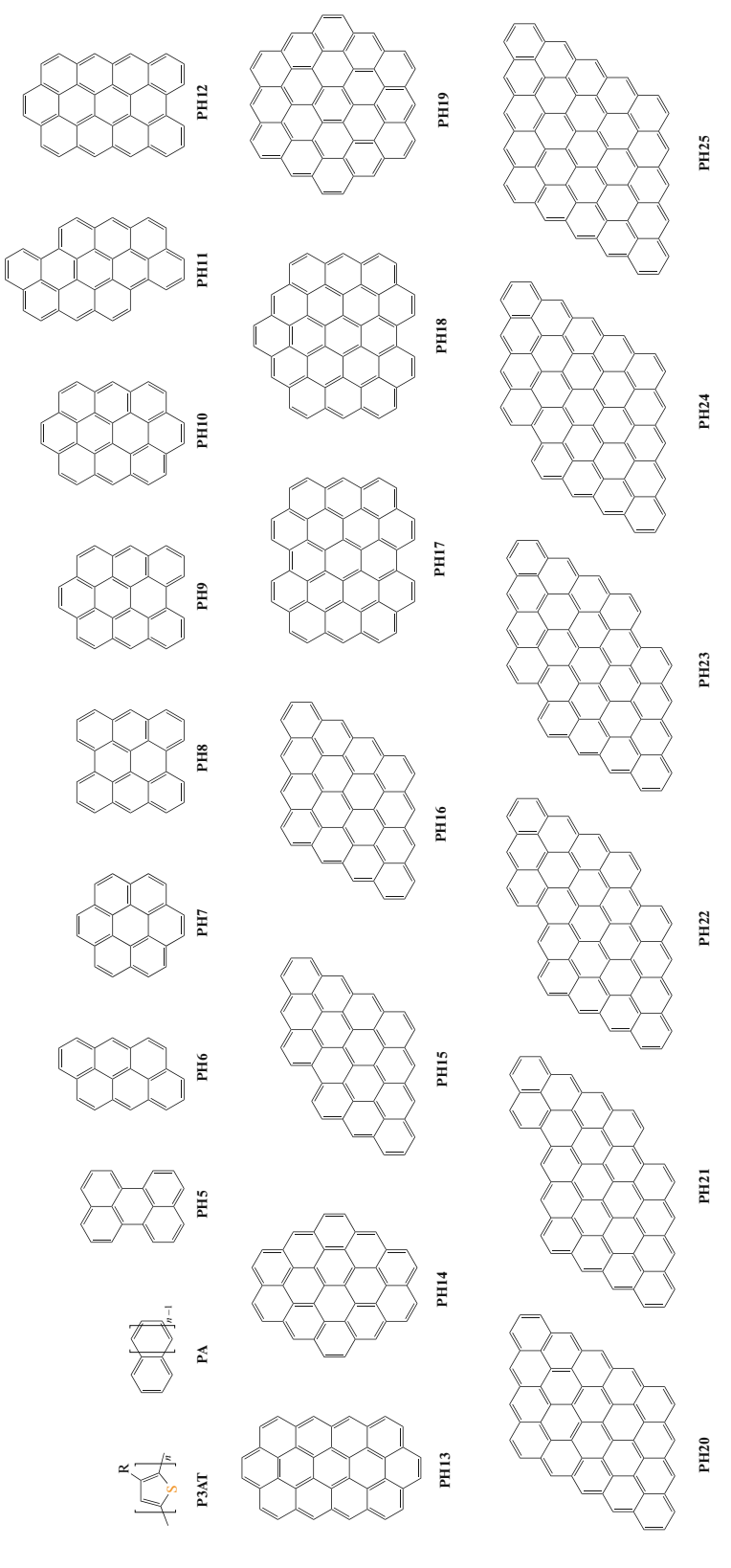

Fig. 1. Oligomers of 3-alkylthiophenes (P3AT): (*1*) poly(3-hydrothiophene) (P3HyT, $m = 0$), (*2*) poly(3-methylthiophene) (P3MeT, $m = 1$), (*3*) poly(3-ethylthiophene) (P3EtT, $m = 2$), (*4*) poly(3-butylthiophene) (P3BuT, $m = 4$), (*5*) poly(3-hexylthiophene) (P3HxT, $m = 6$), (*6*) poly(3-octylthiophene) (P3OcT, $m = 8$), (*7*) poly(3-decylthiophene) (P3DeT, $m = 10$) and (*8*) poly(3-dodecylthiophene) (P3DoT, $m = 12$) examined in this study, as well as quasi-one-dimensional (Q1D) polyacenes (PA) and quasi-two-dimensional (Q2D) graphene-like polycyclic aromatic hydrocarbons (PH) with different numbers of phenyl rings.

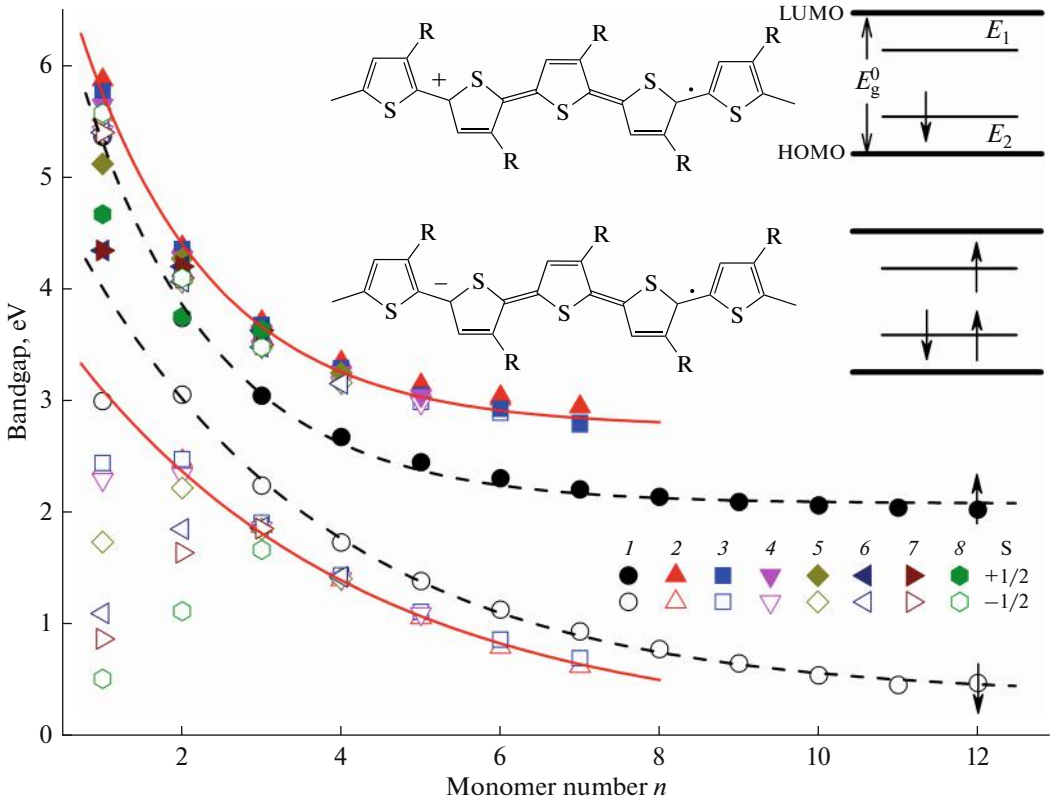

Fig. 2. Dependence of the bandgap $E_g = E_{HOMO} - E_{LUMO}$ of oligomers (*1*) P3HyT, (*2*) P3MeT, (*3*) P3EtT, (*4*) P3BuT, (*5*) P3HxT, (*6*) P3OcT, (*7*) P3DeT, and (*8*) P3DoT with different numbers of monomers n and lengths of alkyl substituents m, optimized using the density functional theory (DFT) in the Mulliken approximation in the Orca environment according to the procedure described in the Methods and Procedures section. The top part sketches the structures of positively and negatively charged polarons on P3AT chains with their corresponding energy sublevels in the oligomer bandgap. The curves illustrate the relationships calculated from Eq. (1) at (from top to bottom) $a_0 = 2.761$ eV, $b = 5.447$ eV, $c = 1.669$; $a_0 = 2.078$ eV, $b = 5.886$ eV, $c = 1.671$; $a_0 = 0.347$ eV, $b = 5.029$ eV, $c = 3.153$; and $a_0 = 0.050$ eV, $b = 4.003$ eV, $c = 3.650$.

The energy parameters HOMO, LUMO, and E_g calculated for neutral and oxidized P3AT oligomers with different numbers of monomers n for both possible polaron spin orientations in an external magnetic field are given in Table 1. The bandgap E_g determined for these compounds is shown in Fig. 2 depending on the number n of their monomers. From the data presented in the figure, one can draw the quite expected conclusion that the E_g value significantly depends both on the number n of the compounds in question and the orientation of the polaron induced in them in an external magnetic field. To a first approximation, the revealed dependences can be described by a simple exponential law

$$a = a_0 + b\exp(-n/c), \quad (1)$$

where a_0 is the value of the sought parameter for an infinite polymer length, i.e. in the limit $n \to \infty$, and b and c are coefficients. From Fig. 2 it follows that the upper and lower $E_g(n)$ relations for the P3HyT oligomer follow the law defined by Eq. (1) with $a_0 =$ 2.078 eV, $b = 5.886$ eV, $c = 1.671$ and $a_0 = 0.347$ eV, $b =$ 5.029 eV, $c = 3.153$, respectively . The upper and lower solid curves calculated from Eq. (1) with $a_0 = 2.761$ eV, $b = 5.447$ eV, $c = 1.669$ and $a_0 = 0.050$ eV, $b = 4.003$ eV, $c = 3.650$, respectively, also well describe the averaged data obtained for the remaining P3ATs with both orientations of their spins. The a_0 values obtained for the studied P3ATs are close to those calculated for P3HyT (2.20 eV) [15] and found experimentally for regioregular P3HxT (1.90–2.07 eV) [17–19], P3OcT (1.92 eV), and P3DeT (1.93 eV) [18].

Thus, the analysis of the data obtained shows that an increase in the degree of polymerization leads to exponential narrowing of the bandgap of conjugated polymers. However, replacing hydrogen atoms in the third position with alkyl chains leads to the opposite effect. This may provide an opportunity to monitor and control charge transfer processes in polymer molecular devices.

Table 1. HOMO, LUMO, and E_g energies (all in eV) calculated for neutral and oxidized 3-alkylthiophene oligomers with different numbers of monomers n, as calculated in the Orca environment according to the procedure described in the Methods and Procedures section

n	HOMO[a]	LUMO[a]	E_g^a	HOMO[b]	LUMO[b]	E_g^b	HOMO[c]	LUMO[c]	E_g^c
	Poly(3-hydrothiophene)								
1	−5.513	−0.501	5.012	−11.923	−6.562	5.362	−12.206	−6.288	5.918
2	−4.951	−1.423	3.528	−9.873	−6.136	3.737	−11.223	−8.172	3.051
3	−4.749	−1.851	2.898	−8.870	−5.828	3.042	−9.732	−7.495	2.237
4	−4.655	−2.094	2.561	−8.246	−5.576	2.670	−8.797	−7.070	1.727
5	−4.608	−2.247	2.361	−7.814	−5.367	2.447	−8.159	−6.778	1.381
6	−4.586	−2.349	2.237	−7.494	−5.192	2.302	−7.692	−6.566	1.126
7	−4.577	−2.420	2.157	−7.246	−5.043	2.204	−7.336	−6.406	0.930
8	−4.576	−2.470	2.106	−7.047	−4.911	2.136	−7.053	−6.281	0.772
9	−4.581	−2.507	2.074	−6.882	−4.792	2.090	−6.824	−6.180	0.644
10	−4.588	−2.534	2.054	−6.741	−4.683	2.059	−6.634	−6.096	0.538
11	−4.597	−2.554	2.043	−6.621	−4.582	2.039	−6.476	−6.025	0.451
12	−4.606	−2.569	2.037	−6.582	−4.561	2.021	−6.381	−5.975	0.406
	Poly(3-methylthiophene)								
1	−5.640	−0.079	5.560	−11.840	−5.969	5.872	−11.853	−9.467	2.386
2	−5.124	−0.960	4.164	−9.880	−5.504	4.376	−10.654	−8.195	2.459
3	−4.923	−1.351	3.572	−8.888	−5.181	3.707	−9.417	−7.545	1.872
4	−4.824	−1.570	3.254	−8.269	−4.926	3.343	−8.531	−7.137	1.394
5	−4.810	−1.722	3.088	−7.867	−4.727	3.139	−7.941	−6.889	1.052
6	−4.855	−1.841	3.014	−7.601	−4.567	3.034	−7.535	−6.745	0.790
7	−4.856	−1.914	2.942	−7.359	−4.415	2.944	−7.213	−6.596	0.616
12*	−4.246	−2.514	1.732	−6.131	−4.335	1.796	−6.030	−5.535	0.495
	Poly(3-ethylthiophene)								
1	−5.590	−0.193	5.397	−11.727	−5.961	5.766	−11.775	−9.336	2.439
2	−5.082	−0.944	4.138	−9.769	−5.415	4.355	−10.550	−8.077	2.472
3	−4.879	−1.344	3.535	−8.782	−5.108	3.673	−9.338	−7.434	1.904
4	−4.781	−1.586	3.195	−8.171	−4.882	3.288	−8.464	−7.032	1.431
5	−4.727	−1.740	2.987	−7.744	−4.696	3.048	−7.860	−6.756	1.104
6	−4.710	−1.821	2.889	−7.434	−4.511	2.923	−7.419	−6.563	0.856
7	−4.689	−1.904	2.785	−7.182	−4.384	2.798	−7.088	−6.399	0.689
	Poly(3-butylthiophene)								
1	−5.604	−0.204	5.400	−11.508	−5.865	5.643	−11.537	−9.246	2.291
2	−5.099	−1.034	4.066	−9.674	−5.394	4.281	−10.340	−8.003	2.337
3	−4.899	−1.420	3.479	−8.703	−5.086	3.617	−9.218	−7.363	1.855
4	−4.795	−1.637	3.158	−8.096	−4.847	3.249	−8.365	−6.964	1.402
5	−4.733	−1.756	2.977	−7.676	−4.633	3.043	−7.780	−6.691	1.089
	Poly(3-hexylthiophene)								
1	−5.595	−0.196	5.399	−10.914	−5.796	5.118	−10.918	−9.188	1.730
2	−5.088	−1.023	4.065	−9.618	−5.347	4.271	−10.173	−7.956	2.217
3	−4.886	−1.408	3.478	−8.654	−5.041	3.613	−9.163	−7.316	1.847
4	−4.785	−1.627	3.158	−8.049	−4.803	3.246	−8.319	−6.917	1.402
	Poly(3-octylthiophene)								
1	−5.590	−0.191	5.399	−10.256	−5.721	4.536	−10.229	−9.136	1.094

Table 1. (Contd.)

n	HOMO[a]	LUMO[a]	E_g^a	HOMO[b]	LUMO[b]	E_g^b	HOMO[c]	LUMO[c]	E_g^c
2	−5.063	−0.999	4.064	−9.566	−5.309	4.257	−9.765	−7.917	1.848
3	−4.868	−1.389	3.479	−8.635	−5.001	3.634	−9.151	−7.291	1.860
4	−4.764	−1.613	3.151	−8.030	−4.770	3.260	−8.312	−6.892	1.420
	Poly(3-decylthiophene)								
1	−5.588	−0.189	5.399	−10.009	−5.665	4.344	−9.965	−9.102	0.864
2	−5.081	−0.985	4.096	−9.502	−5.302	4.200	−9.545	−7.910	1.635
3	−4.872	−1.371	3.500	−8.625	−4.996	3.629	−9.132	−7.282	1.851
	Poly(3-dodecylthiophene)								
1	−5.599	−0.026	5.573	−9.734	−5.066	4.668	−9.555	−9.049	0.506
2	−5.079	−0.983	4.096	−9.032	−5.283	3.748	−9.031	−7.919	1.112
3	−4.872	−1.395	3.478	−8.610	−4.610	3.633	−8.937	−7.276	1.661

[a] Neutral polymer in an aromatic conformation; [b] polymer with a central polaron with a quinoid conformation, charge $+e$ and, spin $S = +1/2$; [c]polymer with a central polaron with a quinoid conformation, charge +1, and spin $S = -1/2$.

Distribution of Spin and Charge Densities in Oligo(3-alkylthiophene)s

Calculations have shown that the formation of a mobile polaron on a P3HyT chain with the quinoid conformation leads not only to a decrease in the polymer bandgap, but also to a decrease in the dihedral/torsion angle S−C=C−S between monomers, as well as the angle −C−S−C− in each monomer. Such structural changes improve the electronic parameters of the polymer and molecular devices based on it. Previously [16], a uniform distribution of spin and charge densities on all constituent atoms within the polaron of this compound was discovered. Replacement of hydrogen atoms in the 3-position of P3AT with hydrocarbon groups significantly alters the properties of the oligomer. This is most clearly demonstrated by analysis of changes in local spin and electronic properties during the transition from the 12-mer P3HyT to P3MeT.

Figure 3 shows the electron density and spin population on each hydrogen, sulfur, and carbon atom of the 12-mer P3MeT that are located along the oligomer main molecular x-axis. For comparison, the dashed lines also show the corresponding parameters obtained for the sulfur atoms of the 12-mer P3HyT. The given data indicate a uniform charge distribution on most P3MeT atoms as in the case of P3HyT. The nature of this distribution also indicates the presence in the oligomer central part of a polaron with a characteristic length of about seven monomers. This parameter is close to that obtained experimentally by measuring EPR [20] and electron-nuclear double resonance (ENDOR) [21] spectra of this polymer.

On the other hand, an analysis of the data presented in Fig. 3 can lead to the conclusion that the spin density is unevenly distributed over all polaron nuclei. Analysis of a simpler dependence of this parameter for ^{32}S in Fig. 3d shows that it consists of at least two contributions, a broad one, apparently corresponding to mobile polarons, and a narrow Gaussian line of less mobile polarons. The existence of the second type of carriers can be explained, for example, by local pinning of part of topological distortions due to the specificity of their formation, relaxation, and interaction with their plastic microenvironment, like that characteristic for some other conjugated compounds of reduced dimensionality [22]. This may be the reason for redistribution of the effective spin density along the main molecular x-axis of the polaron. It should be noted that the existence of an effect of this kind in the 12-mer P3MeT was repeatedly checked in this study. Its accurate interpretation is possible with further investigation of a polymer of this sort, searching through all its side substituents using appropriate equipment. Nevertheless, the data obtained in this work indicate the possible applicability of the proposed procedure for precise control at the atomic level of the structural, conformational, electronic, and spin parameters of various systems based on organic conjugated polymers.

DFT Calculation of Spin Hamiltonian Parameters of Oligo(3-alkylthiophene)s

The spin state and interaction of polarons with their microenvironment in polymer donor–acceptor systems are described by the main parameters of the spin Hamiltonian, the hyperfine coupling (HFC) constant, and the Landé g-factor. Table 2 presents the main values of the hyperfine coupling tensors of polaron spins with ^{1}H atoms, A, and the Landé factor of the interaction of polaron spins with an external magnetic field, g, as well as their averaged/isotropic values, A_{iso} and g_{iso}, respectively, calculated for spin charge carriers in the studied oxidized oligo(3-alkylth-

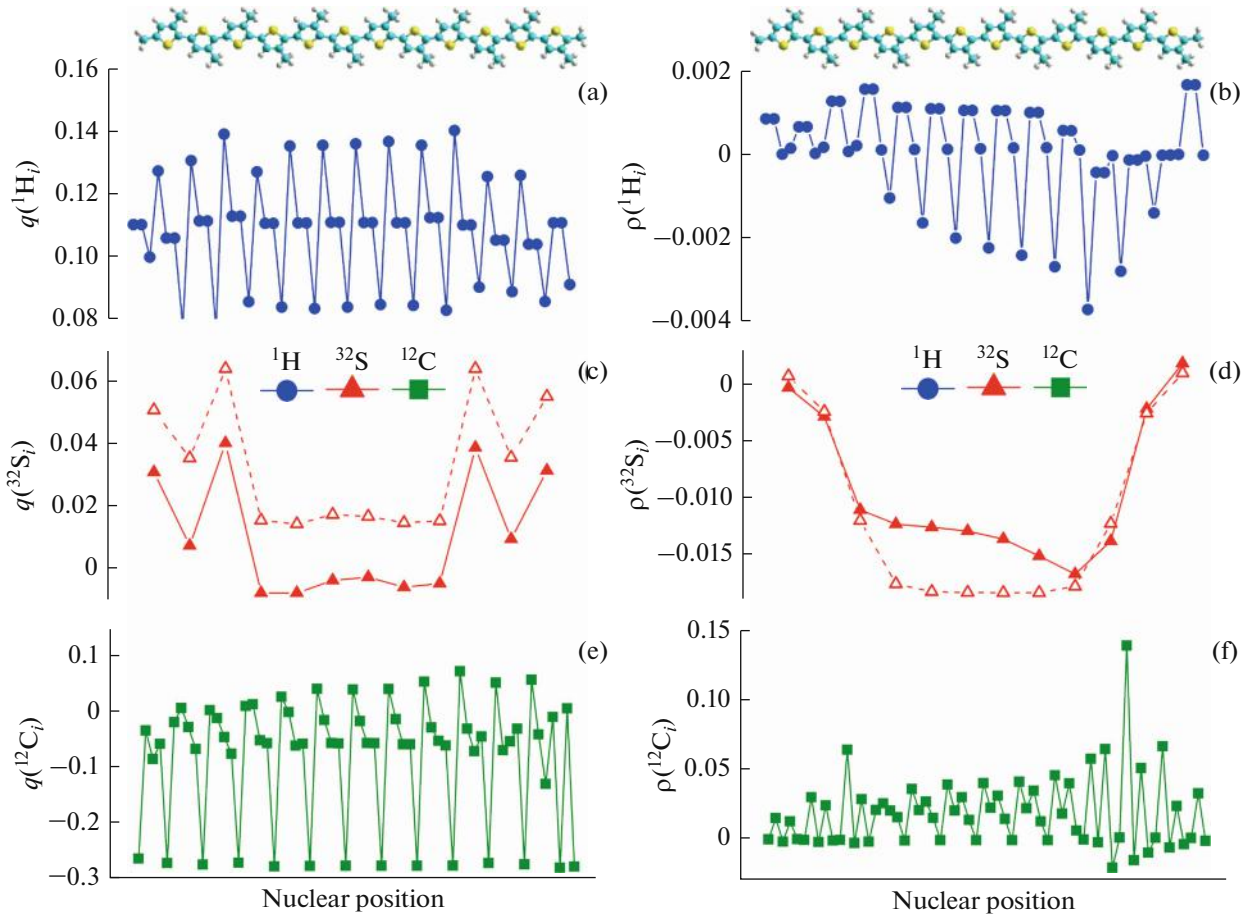

Fig. 3. Relative change in (a, c, e) charge and (b, d, f) spin densities on the hydrogen ^1H (circles), sulfur ^{32}S (triangles), and carbon ^{12}C (squares) nuclei located along the main *x*-axis within the polaron of the oxidized 12-mer of 3-methylthiophene (schematically shown above), optimized in terms of the density functional theory, calculated using the Mulliken method in the Orca environment according to the procedure described in the Methods and Procedures section. For comparison, open triangles in (c, d) show the corresponding parameters previously calculated for the sulfur atoms of the P3HyT oligomer [16].

iophene)s. Analysis of these data may indicate the dependence of both tensors of the spin Hamiltonian of the oligomers on the structure of their side alkyl substituents and the degree of polymerization *n*. Figure 4 shows the parameters A_{iso} and g_{iso} plotted against the number *n* of monomer units in the studied oligomers. These plots can also be approximated by Eq. (1). Indeed, the parameters presented in the figure, calculated for the polarons of the P3HyT oligomer, change according to the aforementioned exponential law with $a_0 = 0.471$ MHz, $b = 83.62$ MHz, $c = 1.17$ and $a_0 = 2.00162$, $b = 8.71 \times 10^{-4}$, $c = 5.31$, respectively , while the same parameters of the remaining P3AT obey Eq. (1) with averaged coefficients of $a_0 = 1.873$ MHz, $b = 81.31$ MHz, $c = 0.976$ and $a_0 = 2.00189$, $b = 6.41 \times 10^{-4}$, $c = 2.79$, respectively (Fig. 4). This is evidence for an increase in HFC and an increase in the magnetic moment of polarons due to the replacement of P3AT protons in the third position by corresponding alkyl substituents.

The anisotropic HFC constants and *g*-factor obtained for the studied P3AT oligomers in the $n \to \infty$ limit were then used to calculate their high-resolution D-band EPR spectra ($\nu_e = 140$ GHz, $B_0 = 4996$ mT) using the EasySpin software. In this case, the different nature of spectral broadening for these compounds was taken into account. As is known, spectral broadening can be due to various dynamic and static effects arising as a result of orientational disorder and/or unresolved HFC. Such effects are initiated by structural changes in the microenvironment of polarons induced in a disordered system and therefore depend on the polaron orientation relative to the external magnetic field. Thus, to calculate the EPR spectra of the compounds in question, the corresponding tensors *A* and *g* characterized by the so-called *B*- and *g*-strains were used. For example, when calculating the EPR spectrum of the quinoid conformer of the 12-mer P3HyT, the matrices [0.270 1.178 1.524] MHz and [0.0005 0.0004 0.0005], respectively, were used. The EPR spectra calculated for some P3AT oligomers

Table 2. The principal values of the hyperfine coupling tensors of ^{1}H atoms, A_i (in MHz), the Landé g-factor of the interaction of polaron spins with an external magnetic field, and their average/isotropic values A_{iso} and g_{iso}, respectively, calculated for oxidized 3-alkylthiophene oligomers with different numbers of monomers n in the Orca environment according to the procedure described in the Methods and Procedures section

n	A_x	A_y	A_z	A_{iso}	g_{xx}	g_{yy}	g_{zz}	g_{iso}
				Poly(3-hydrothiophene)				
1	34.826	32.965	37.999	35.263	2.001279	2.002066	2.002730	2.002025
2	14.877	12.252	14.206	13.778	2.003815	2.002006	2.000769	2.002197
3	7.172	5.460	6.109	6.247	2.002979	2.002012	2.001398	2.002130
4	4.219	2.028	2.521	2.923	2.003111	2.002021	2.001000	2.002044
5	2.632	0.491	0.562	1.228	2.002906	2.002014	2.000970	2.001963
6	1.704	−0.328	−0.478	0.299	2.002944	2.002007	2.000741	2.001898
7	1.168	−0.743	−1.021	−0.199	2.002857	2.001999	2.000651	2.001836
8	0.819	−0.968	−1.313	−0.487	2.002867	2.001993	2.000528	2.001796
9	0.590	−1.081	−1.451	−0.647	2.002835	2.001975	2.000488	2.001766
10	0.431	−1.133	−1.505	−0.736	2.002854	2.001930	2.000443	2.001742
11	0.332	−1.134	−1.502	−0.768	2.002835	2.001933	2.000443	2.001736
12	0.270	−1.178	−1.524	−0.811	2.00283	2.00191	2.00043	2.001723
				Poly(3-methylthiophene)				
1	30.508	31.452	38.383	33.448	2.003308	2.002041	2.001236	2.002195
2	12.618	12.401	15.871	13.630	2.003305	2.002002	2.001172	2.002160
3	6.861	6.405	8.530	7.265	2.002972	2.002004	2.001382	2.002119
4	4.355	3.866	5.339	4.520	2.003060	2.001993	2.001157	2.002070
5	3.083	2.620	3.736	3.146	2.002985	2.001961	2.001115	2.002020
6	2.417	1.992	2.894	2.434	2.002977	2.001916	2.000967	2.001953
7	1.953	1.566	2.320	1.946	2.002946	2.001946	2.000947	2.001946
				Poly(3-ethylthiophene)				
1	27.088	27.304	32.247	28.880	2.002888	2.002034	2.001358	2.002093
2	9.541	9.548	11.644	10.245	2.003282	2.002016	2.001110	2.002136
3	4.643	4.400	5.742	4.928	2.002964	2.002088	2.001295	2.002116
4	2.660	2.449	3.194	2.768	2.003035	2.002026	2.001113	2.002058
5	1.683	1.545	1.914	1.714	2.002966	2.001949	2.001038	2.001984
6	1.179	0.934	1.315	1.143	2.002980	2.001946	2.000991	2.001972
7	1.331	1.105	1.479	1.306	2.002953	2.001944	2.001006	2.001968
				Poly(3-butylthiophene)				
1	17.260	17.312	20.399	18.324	2.003063	2.001961	2.001322	2.002115
2	5.769	5.511	7.394	6.225	2.003443	2.002091	2.001130	2.002221
3	2.700	2.609	3.539	2.949	2.003445	2.002065	2.000959	2.002156
4	1.527	1.477	1.968	1.657	2.003221	2.002016	2.000959	2.002065
				Poly(3-hexylthiophene)				
1	13.143	14.242	15.419	14.268	2.003134	2.001991	2.001333	2.002153
2	4.331	4.114	5.632	4.692	2.003448	2.002072	2.001140	2.002220
3	2.017	1.861	2.716	2.180	2.003450	2.002063	2.000966	2.002160
				Poly(3-octylthiophene)				
1	9.909	10.424	11.088	10.474	2.003195	2.002008	2.001339	2.002181
2	3.172	3.027	4.079	3.426	2.003324	2.002109	2.001069	2.002167
3	1.598	1.469	2.057	1.708	2.002896	2.002107	2.001296	2.002099

Table 2. (Contd.)

n	A_x	A_y	A_z	A_{iso}	g_{xx}	g_{yy}	g_{zz}	g_{iso}
	Poly(3-decylthiophene)							
1	9.068	9.454	9.966	9.496	2.003258	2.002058	2.001358	2.002225
2	2.875	2.735	3.785	3.131	2.003325	2.002110	2.001071	2.002169
	Poly(3-dodecylthiophene)							
1	5.889	5.609	5.810	5.770	2.003601	2.002330	2.001646	2.002526
2	2.474	2.349	3.263	2.695	2.003500	2.002050	2.001186	2.002245

* The principal values of the A- and g-tensors may not coincide.

using the data summarized in Table 2 are also presented in the inset in Fig. 4. From this figure it follows that both parameters A_{iso} and g_{iso} of the studied oligomers monotonically decrease with an increase in the length of their side alkyl substituents m and the number of monomers n. However, there is no such monotony of the shape change in the EPR spectra of these compounds. This discrepancy may result from different conformations of their monomers and thus different configurations and/or spin cloud densities of their charge carriers, which appear in the case of enhancement of intermolecular interactions in real polymers and their composites. The magnetic resonance parameters calculated in this study differ from those calculated or experimentally obtained for graphene [23]; however, they turned out to be close to those determined experimentally for the initial and modified P3AT [12, 18, 24–27].

Calculation of Structural and Magnetic Properties of Oligo(3-alkylthiophene)s Modified with Polycyclic Aromatic Hydrocarbon Molecules

Preliminary studies [8, 9] have shown that additions of small molecules with a π-conjugated structure

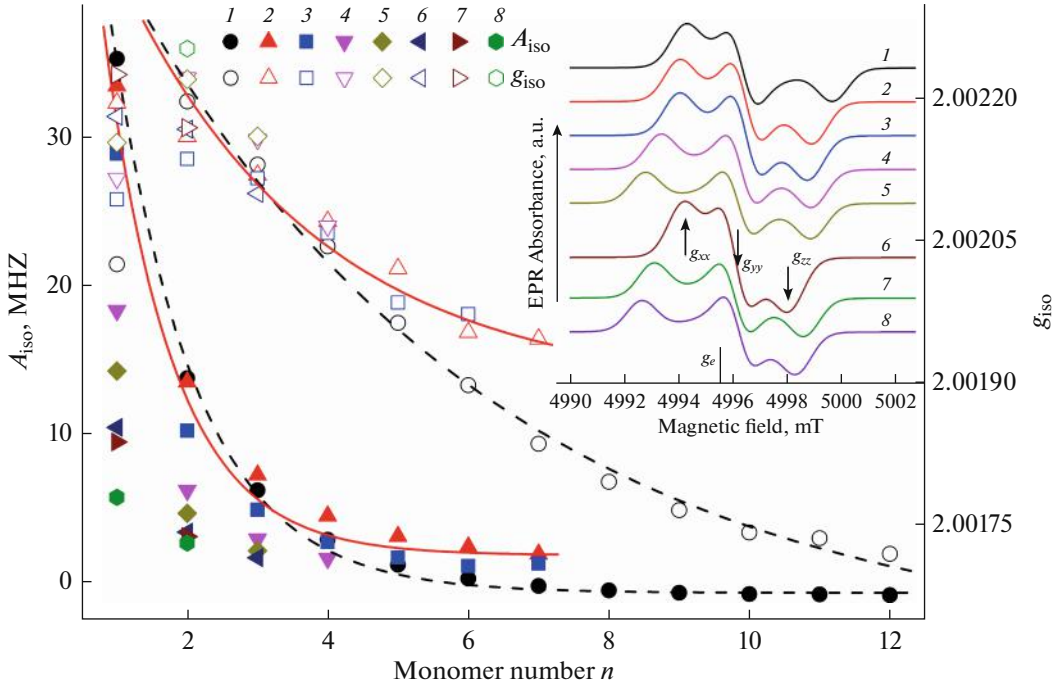

Fig. 4. Dependence of isotropic spin–spin hyperfine coupling constants A_{iso} and g-factor g_{iso} of polaron charge carriers induced on (*1*) P3HyT, (*2*) P3MeT, (*3*) P3EtT, (*4*) P3BuT, (*5*) P3HxT, (*6*) P3OcT, (*7*) P3DeT, and (*8*) P3DoT oligomer chains on the number n of their monomer units and the length m of their alkyl substituents, optimized and calculated in the Orca software according to the procedure described in the Methods and Procedures section. The inset shows the D-band EPR spectra of polarons calculated using the EasySpin program and the A_{iso} and g_{iso} parameters listed in Table 2 for these oligomers. The upper and lower solid curves refer to the relationships calculated from Eq. (1) with $a_0 = 2.00162$, $b = 8.71 \times 10^{-4}$, $c = 5.31$ and $a_0 = 0.471$ MHz, $b = 83.62$ MHz, $c = 1.17$, respectively, and the dashed upper and lower curves show the relations calculated from the same equation with $a_0 = 2.00189$, $b = 6.41 \times 10^{-4}$, $c = 2.79$ and $a_0 = 1.873$ MHz, $b = 81.31$ MHz, $c = 0.976$, respectively.

significantly improve the structural and electronic–dynamic properties of polymer composites. It turned out that such additives play the role of growth points for the crystalline phase of the polymer matrix of composites, which reduces both the number of spin traps induced in it and the probability of recombination of spin charge carriers. Below are the results of a study on the possibility of using additional control over such parameters of the studied oligomers with the use of more extended Q1D polyacenes and Q2D graphene-like polyaromatic hydrocarbons.

Table 3 shows the main energy parameters HOMO, LUMO, and E_g calculated for composites of P3HyT and P3MeT 7-mers with polycyclic aromatic additives PA and PH having different numbers of benzene rings n (see Fig. 1) for both spin orientations of the induced polaron relative to the external magnetic field. Similar parameters of neutral additives are given in Table 4. As an example, a change in the bandgap of the P3HyT composite depending on the number n of both polycyclic additives is shown in Fig. 4a. From the data presented it can be seen that the E_g value of the oligomer, as expected, decreases monotonically in the case of its complex with PA with a small number (2–3) of its conjugated rings. Previously, a similar effect was experimentally revealed in the study of photovoltaic complexes based on P3DoT [8, 9] and other conjugated polymers [28]. Therefore, it would be quite logical to expect a further monotonic decrease in the energy E_g in the limit $n \to \infty$. However, this turned out not to be the case. It was found that the E_g value of composites of both oligomers containing PA and PH additives changes in a variable manner for $n > 3$ and both polaron spin orientations relative to the direction of the external magnetic field. It should be noted that this effect is more pronounced in the case of P3HyT used as a composite matrix and PH as a Q2D nanoadditive. Analyzing the obtained data presented in Fig. 5a, one can notice the presence of specific periodicity in the change in the function $E_g(n)$ with the "period" close to $\Delta n \approx 4$. This "effect" is somewhat reduced in complexes with the P3MeT oligomer as a matrix. A slight deviation of the extrema of this dependence can be caused by the scatter in the orientations of the planes of polymer chains and additives and by the structural molecular asymmetry of PH molecules. An attempt can be made to search for a possible relationship between the structural, electronic, and spin parameters of the complexes under study. Figure 5b shows changes in the spin density on sulfur atoms, $\rho(^{32}S_c) - \rho(^{32}S_c^0)$, of the same complex with varying the number n of conjugated rings of polycyclic aromatic additives PA and PH. The choice of this parameter for such an analysis is due to greater simplicity of its further interpretation due to the least interaction of sulfur atoms with their microenvironment. Indeed, if the polaron spin interacted with the sulfur nucleus, similar to its interaction, for example, in the benzo-1,2,3-trithiol radical cation, then the g-factor of the corresponding compound would be $g_s = 2.0144–2.0197$ [29], which is significantly higher than that of spin charge carriers of the studied oligomers and other organic compounds. An analysis of the change in spin density on the sulfur atoms of the composite also revealed its nontrivial dependence on the size of both nanoadditives. The composite is also characterized by approximately equidistant extrema of the dependences of $\rho(^{32}S_c)$ on n with a distance between them $\Delta n \approx 4$. However, the "extrema" of this dependence do not coincide with those of $E_g(n)$. Figure 5c presents the plots of the bandgap of PA and PH nanoadditives. The Q2D graphene is known a priori to have no bandgap; that is, $E_g = 0$ at $n \to \infty$. However, a bandgap with a width typical of dielectrics and wide-gap semiconductors can be formed between the valence and conduction bands of some graphene-like Q2D films of limited size. For example, the E_g value of graphene oxide can vary in the range of 1.7–2.7 eV depending on the degree of modification [30]. Additionally, this parameter may become nonzero when the Q2D sample changes to the chair configuration. Extrapolation of this PA parameter gives $E_g = 0.53$ eV at $n \to \infty$ (see Fig. 5c); that is, the configuration is intermediate. An interesting fact was the change in $E_g(n)$ of isolated PH molecules with a periodicity of about 4 phenyl rings, possibly due to their Q2D structural degeneracy, which was not manifested in the case of Q1D PA molecules. Note that in this work, the manifestation of the described unusual effects was confirmed by several repeated calculations.

Analysis of the data in Fig. 5 leads to a number of important conclusions. First, small aromatic additives do affect the spin population/density of central polarons, and this interaction is most significant in P3HyT-based composites. This effect is explained by the shielding of the π-interaction of molecular additives with chains of other oligomers, the side alkyl substituents of which act as an inhibitor of intermolecular interaction. Second, as in the case of bandgap, the studied composites are also characterized by a specific "periodic" change in the spin density $\rho(3^2Sc)$ with varying the number of phenyl rings n. Comparison of the data shown in Fig. 5 allows for the third, main conclusion about both the correlated change in the bandgaps of polymer composites and Q2D nanoadditives and their antibatic behavior with the parameter $\rho(^{32}Sc)$ of polymer composites. This fact should clearly indicate structural and electronic rearrangements induced in oligomers by such nanoadditives with a periodic molecular π-conjugated structure. This feature can be used, for example, in the development of molecular spintronic linear (at small values of n) and selective (at $n \geq 4$) sensors and filters with spin-dependent external control of electronic parameters.

Table 4 shows the main values of the A- and g-tensors and their isotropic values A_{iso} and g_{iso} calculated

Table 3. HOMO, LUMO, and E_g energies (all in eV) calculated for the initial 7-mers of 3-hydrothiophene and 3-methylthiophene (Init) and the same oligomers, modified with additives (Adds) of π-conjugated polyacenes (PA*n*) and polycyclic aromatic hydrocarbons (PH*n*) with different numbers of benzene rings *n*, in the Orca environment according to the procedure described in the Methods and Procedures section

Adds	HOMO[a]	LUMO[a]	E_g^a	HOMO[b]	LUMO[b]	E_g^b	HOMO[a]	LUMO[a]	E_g^a	HOMO[b]	LUMO[b]	E_g^b
	Poly(3-hydrothiophene)						Poly(3-methylthiophene)					
Init	–6.961	–5.132	1.829	–7.194	–6.075	1.118	–6.672	–4.810	1.862	–6.900	–5.772	1.128
PA1	–6.918	–5.095	1.823	–7.163	–6.025	1.137	–6.637	–4.779	1.858	–6.876	–5.732	1.144
PA2	–6.875	–5.064	1.812	–7.131	–5.986	1.145	–6.609	–4.760	1.850	–6.860	–5.703	1.157
PA3	–6.867	–5.053	1.818	–7.012	–5.971	1.041	–6.593	–4.749	1.844	–6.841	–5.688	1.153
PA4	–6.712	–4.992	1.720	–6.792	–5.899	0.893	–6.530	–4.724	1.806	–6.665	–5.657	1.008
PA5	–6.409	–5.008	1.401	–6.400	–5.894	0.506	–6.346	–4.753	1.594	–6.342	–5.656	0.686
PA6	–6.562	–4.890	1.672	–6.472	–5.809	0.663	–6.398	–4.652	1.747	–6.366	–5.587	0.779
PA7	–6.383	–4.912	1.470	–6.387	–5.823	0.564	–6.338	–4.638	1.699	–6.262	–5.574	0.688
PA8	–6.375	–4.881	1.494	–6.332	–5.785	0.547	–6.285	–4.617	1.669	–6.271	–5.550	0.720
PA9	–6.329	–4.870	1.459	–6.258	–5.763	0.495	–6.256	–4.597	1.659	–6.257	–5.539	0.718
PA10	–6.286	–4.860	1.426	–6.257	–5.759	0.498	–6.017	–5.467	0.550	–6.250	–4.976	1.274
PH5	–6.810	–4.998	1.813	–6.798	–5.921	0.877	–6.602	–4.700	1.902	–6.758	–5.713	1.044
PH6	–6.737	–4.987	1.750	–6.728	–5.934	0.793	–6.542	–4.700	1.842	–6.690	–5.638	1.052
PH7	–6.811	–4.988	1.822	–7.059	–5.913	1.146	–6.559	–4.693	1.865	–6.786	–5.649	1.137
PH8	–6.514	–5.085	1.429	–6.405	–5.788	0.617	–6.369	–4.700	1.669	–6.357	–5.637	0.719
PH9	–6.564	–4.958	1.606	–6.547	–5.882	0.665	–6.459	–4.667	1.792	–6.454	–5.623	0.831
PH10	–6.774	–4.987	1.787	–6.780	–5.883	0.897	–6.540	–4.670	1.870	–6.718	–5.631	1.087
PH11	–6.497	–4.884	1.613	–6.462	–5.828	0.634	–6.488	–4.633	1.855	–6.638	–5.591	1.047
PH12	–6.464	–4.972	1.492	–6.380	–5.774	0.607	–6.204	–4.750	1.454	–6.190	–5.581	0.609
PH13	–6.497	–4.884	1.613	–6.462	–5.827	0.635	–6.352	–4.638	1.714	–6.352	–5.592	0.760
PH14	–6.583	–4.920	1.663	–6.584	–5.843	0.740	–6.508	–4.641	1.867	–6.551	–5.590	0.961
PH15	–6.349	–4.877	1.472	–6.323	–5.755	0.568	–	–	–	–	–	–
PH16	–6.323	–4.843	1.480	–6.311	–5.790	0.521	–	–	–	–	–	–
PH17	–6.542	–4.944	1.598	–6.534	–5.840	0.694	–	–	–	–	–	–
PH18	–6.620	–4.939	1.681	–6.614	–5.836	0.778	–	–	–	–	–	–
PH19	–6.657	–4.902	1.755	–6.695	–5.823	0.872	–	–	–	–	–	–
PH20	–6.291	–4.814	1.477	–6.313	–5.747	0.566	–	–	–	–	–	–

for some composites, which were used to simulate the corresponding EPR spectra in the EasySpin software. The inset in Fig. 5b exemplifies the D-band EPR spectra of the P3HyT : PA1 and P3MeT : PA1 composites, as calculated using the magnetic resonance parameters obtained for them.

CONCLUSIONS

In this work, the energy and spin parameters were calculated for P3AT oligomers with different structures, conformations, and spin states of polymer chains and for their complexes with various aromatic Q1D and Q2D polycyclic hydrocarbons. The results

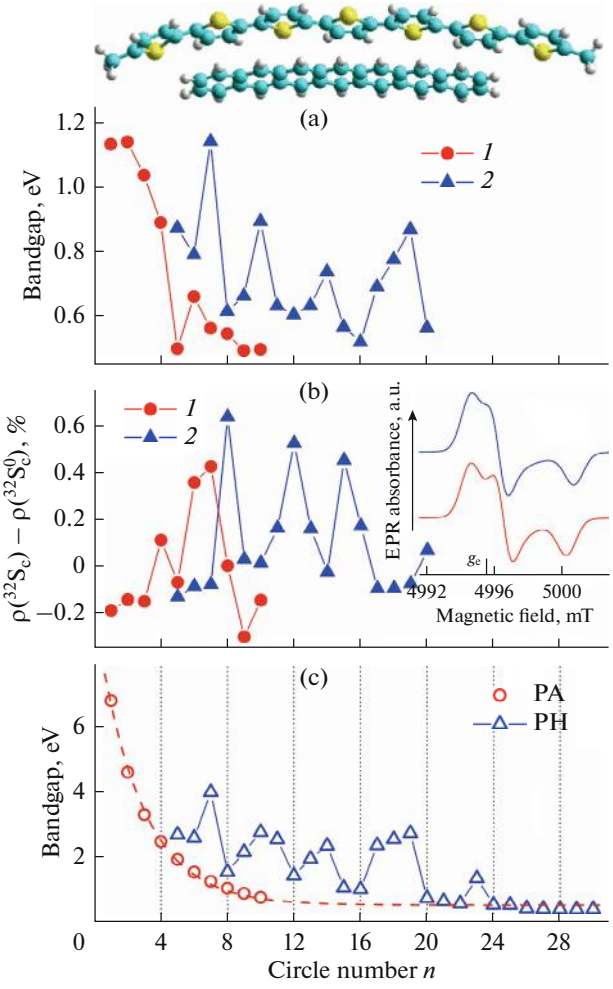

Fig. 5. (a) Change in the bandgap of the 7-mer complex (*1*) P3HyT:PA and (*2*) P3HyT : PH depending on the number of phenyl rings n. (b) Spin density on ^{32}S nuclei within the extended polaron of the (*1*) P3HyT : PA and (*2*) P3HyT : PH composites as a function of n; in the inset, the upper and lower curves show the D-band EPR spectra of the P3HyT : PA1 and P3MeT : PA1 complexes, respectively, calculated using the data in Table 4. (c) Bandgap of aromatic Q1D PA and Q2D PH molecules depending on the number n of their phenyl rings. The dashed curve refers to the relation calculated from Eq. (1) with $a_0 = 0.532$ eV, $b = 8.968$ eV, and $c = 2.647$. The top panel shows an example of a structurally optimized P3HyT : PA7 complex.

obtained made it possible to reveal exponential narrowing of the bandgap of the oligomers with increasing degree of polymerization. However, replacing hydrogen atoms in the third position of P3AT monomers with alkyl chains leads to the opposite result. The charge and spin densities on each atom of the studied oligomers and their composites were calculated separately. The localization of some topological spin distortions due to the specificity of their formation, relaxation, and interaction with their microenvironment was identified. This suggested the coexistence of mobile and trapped polarons in P3AT. A relationship was discovered between the electronic and spin properties of composites of the oligomers with polyaromatic π-additives and the molecular structure of the latter. It has been shown that the interaction of Q1D polymer chains with Q1D and Q2D molecules initiates the molecular self-ordering of the composite. This makes it possible to control its morphology and, consequently, its electronic and spin properties. A discrete change in these parameters with an change in the number of rings of aromatic Q2D additives was revealed. Complete sets of anisotropic parameters of the spin Hamiltonians of the studied oligomers and their composites were obtained at different degrees of their polymerization, as well as the structures of their side alkyl substituents and aromatic nanoadditives. High-resolution EPR spectra of these compounds have been calculated.

The methods and approaches proposed in this work for tuning structural and electronic parameters can become key factors in the study of a wide range of polymer donor–acceptor compounds and the design on their basis of various high-performance nanoelectronic devices with graphene-supported spin-dependent electronic parameters.

ABBREVIATIONS

P3AT	poly(3-alkylthiophene)
P3HyT	poly(3-hydrothiophene)
P3MeT	poly(3-methylthiophene)
P3EtT	poly(3-ethylthiophene)
P3BuT	poly(3-buthylthiophene)
P3HxT	poly(3-hexylthiophene)
P3OcT	poly(3-octylthiophene)
P3DeT	poly(3-decylthiophene)
P3DoT	poly(3-dodecylthiophene)
PA	polyacenes
PH	polycyclic hydrocarbons
DFT	density functional theory
EPR	electron paramagnetic resonance
Q1D	quasi-one-dimensional
Q2D	quasi-two-dimensional
HOMO	higher occupied molecular orbital
LUMO	lower unoccupied molecular orbital
X-mer	oligomer composed of *X* monomers
HFC	hyperfine coupling

FUNDING

The work was carried out within the state assignment framework, state registration no. AAAA-A19-119032690060-9 / FFSG-2024-0010.

Table 4. Principal and averaged/isotropic values of the spin–spin hyperfine coupling tensors A (all in MHz) and g-tensors calculated for some initial 7-mers of 3-hydrothiophene (P3HyT) and 3-methylthiophene (P3MeT) and their complexes (Complex) with polyacenes (PAn) using the Orca software according to the method described in the Methods and Procedures section

Complex	A_x	A_y	A_z	A_{iso}	g_{xx}	g_{yy}	g_{zz}	g_{iso}
P3HyT	1.168	–0.743	–1.021	–0.199	2.002857	2.001999	2.000651	2.001836
P3HyT : PA1	1.244	–0.411	–0.822	0.004	2.002746	2.002058	2.000272	2.001692
P3HyT : PA2	1.186	–0.333	–0.629	0.075	2.002745	2.002050	2.000318	2.001705
P3HyT : PA3	1.164	–0.371	–0.689	0.035	2.002756	2.002049	2.000320	2.001708
P3MeT	1.953	1.566	2.320	1.946	2.002946	2.001946	2.000947	2.001946
P3MeT : PA1	1.293	0.827	0.897	1.005	2.002747	2.001948	2.000445	2.001713

CONFLICT OF INTEREST

The authors declare no conflict of interest.

REFERENCES

1. *Organic Optoelectronics*, Hu, W., ed., Weinheim: Wiley–VCH, 2013.
2. Khalifeh, S., *Polymers in Organic Electronics: Polymer Selection for Electronic, Mechatronic, and Optoelectronic Systems*, Toronto: ChemTec, 2020.
3. Zdyb, A., *Third Generation Solar Cells*, Boca Raton: Routledge, 2023.
4. Ganesamoorthy, R., Sathiyan, G., and Sakthivel, P., *Sol. Energy Mater. Sol. Cells*, 2017, vol. 161, p. 102.
5. Sauvé, G., *Chem. Rec.*, 2019, vol. 19, no. 6, p. 1078.
6. Krinichnyi, V.I., *Multi Frequency EPR Spectroscopy of Conjugated Polymers and Their Nanocomposites*, Boca Raton: CRC, 2016.
7. Niklas, J. and Poluektov, O.G., *Adv. Energy Mater.*, 2017, vol. 7, no. 10, p. 1602226.
8. Krinichnyi, V.I., Yudanova, E.I., Denisov, N.N., and Bogatyrenko, V.R., *Synth. Met.*, 2020, vol. 267, p. 116462.
9. Krinichnyi, V.I., Yudanova, E.I., and Denisov, N.N., *J. Phys. Chem. C*, 2022, vol. 126, no. 9, p. 4495.
10. Neeze, F., *WIREs Comput. Mol. Sci.*, 2012, vol. 2, no. 1, p. 73.
11. Mulliken, R.S., *J. Chem. Phys.*, 1955, vol. 23, no. 12, p. 2343.
12. Van Landeghem, M., Maes, W., Goovaerts, E., and Van Doorslaer, S., *J. Magn. Reson.*, 2018, vol. 288, p. 1.
13. Hanwell, M.D., Curtis, D.E., Lonie, D.C., Vandermeersch, T., Zurek, E., and Hutchison, G.R., *J. Cheminform.*, 2012, vol. 4, no. 1, p. 17.
14. Stoll, S. and Schweiger, A., *J. Magn. Reson.*, 2006, vol. 178, no. 1, p. 42.
15. Brédas, J.L., Themans, B., Fripiat, J.G., Andre, J.M., and Chance, R.R., *Phys. Rev. B: Condens. Matter*, 1984, vol. 29, no. 12, p. 6761.
16. Krinichnyi, V.I., *High Energy Chem.*, 2023, vol. 58, no. 1, p. 166.
17. Kim, D.H., Park, Y.D., Jang, Y.S., Yang, H.C., Kim, Y.H., Han, J.I., Moon, D.G., Park, S.J., Chang, T.Y., Chang, C.W., Joo, M.K., Ryu, C.Y., and Cho, K.W., *Adv. Funct. Mater.*, 2005, vol. 15, no. 1, p. 77.
18. Sensfuss, S. and Al-Ibrahim, M., *Organic Photovoltaics: Mechanisms, Materials, and Devices*, Sun, S.S. and Sariciftci, N.S., Eds., Boca Raton: CRC, 2005, p. 529.
19. Enengl, C., Enengl, S., Pluczyk, S., Havlicek, M., Lapkowski, M., Neugebauer, H., and Ehrenfreund, E., *ChemPhysChem*, 2016, vol. 17, no. 23, p. 3836.
20. Devreux, F., Genoud, F., Nechtschein, M., and Villeret, B., *Electronic Properties of Conjugated Polymers*, vol. 76 of *Springer Series in Solid-State Sciences*, Kuzmany, H., Mehring, M., and Roth, S., Berlin: Springer, 1987, p. 270.
21. Kuroda, S., Marumoto, K., Sakanaka, T., Takeuchi, N., Shimoi, Y., Abe, S., Kokubo, H., and Yamamoto, T., *Chem. Phys. Lett.*, 2007, vol. 435, nos. 4–6, p. 273.
22. Brazovskii, S. and Nattermann, T., *Adv. Phys.*, 2004, vol. 53, no. 2, p. 177.
23. Shrestha, A., Higuchi, K., Yoshida, S., and Higuchi, M., *J. Appl. Phys.*, 2021, vol. 130, no 12, p. 124303.
24. Bernier, P., *Handbook of Conducting Polymers*, Scotheim, T.A., Ed., New York: Marcel Dekker, 1986, vol. 2, p. 1099.
25. Aguirre, A., Gast, P., Orlinskii, S., Akimoto, I., Groenen, E.J.J., El Mkami, H., Goovaerts, E., and Van Doorslaer, S., *Phys. Chem. Chem. Phys.*, 2008, vol. 10, no. 47, p. 7129.

26. Konkin, A., Ritter, U., Scharff, P., Roth, H.-K., Aganov, A., Saricifci, N.S., and Egbe, D.A.M., *Synth. Met.*, 2010, vol. 160, nos. 5–6, p. 485.

27. Krinichnyi, V.I., *Spectroscopy of Polymer Nanocomposites*, Thomas, S., Rouxel, D., and Ponnamma, D., Eds., Amsterdam: Elsevier, 2016, p. 202.

28. Krinichnyi, V.I., Yudanova, E.I., Denisov, N.N., Konkin, A.A., Ritter, U., Bogatyrenko, V.R., and Konkin, A.L., *J. Phys. Chem. C*, 2021, vol. 125, no. 22, p. 1224.

29. Krinichnyi, V.I., Herrmann, R., Fanghanel, E., Morke, W., and Luders, K., *Appl. Magn. Reson.*, 1997, vol. 12, nos. 2–3, p. 317.

30. Jeong, H.K., Jin, M.H., So, K.P., Lim, S.C., and Lee, Y.H., J. *Phys. D: Appl. Phys.*, 2009, vol. 42, no. 6, p. 065418.

Translated by S. Zatonsky